# Accurate cogging and linear ripple models for parametrized Feed Forward

## A method for splitting up motor ripple into current independent and current dependent fractions

Dr. Ir. T.L. van Vuure
R&D department
Tecnotion B.V.
Almelo, The Netherlands
Thorwald.van.Vuure@Tecnotion.com

M. Kuiper
Applied Physics
Saxion
Enschede, The Netherlands
mattijskuiper94@hotmail.com

***Abstract*—In Iron Core Motors, there are two types of ripple – i.e. position dependent, current dependent parasitic forces. One is only marginally dependent on current (the detent force) and the other is linear with current. Clearly, for formulating accurate detent force models for the purpose of successfully utilizing parametrized Feed Forward techniques it will be crucial to independently determine both fractions of the total ripple. A technique is presented which accomplishes this, both in simulation and in measurement. The potential benefit for a parametrized Feed Forward system is illustrated.**

***Keywords—Feed Forward; Cogging, Detent Force, Ripple***

## I. INTRODUCTION

In PMLSMs, Permanent Magnet Linear Synchronous Motors, there is a big practical difference between Iron Core and Ironless (or Coreless, or Air Core) motors: the latter type is more suitable for applications that require a low velocity ripple. The reason for this practical difference is assumed to be the lower force ripple, i.e. the variation in motor force for a given current as a function of position. However: there is often no great difference in overall motor ripple. The qualitative difference between the two motor types and their respective types of ripple is explained in section II.

Ironless motors, though preferable in terms of their ripple, as discussed below, are considerably more expensive per unit length of the magnet way. Short stroke applications can easily pay this price. For long stroke applications, compensating ripple with parametrized feed-forward is an area of active interest. [1][2]

## II. RIPPLE COMPONENTS

Both Iron Core and Ironless motors show a position dependent variation in the motor force, which can be explained from the fact that the magnetic field distribution from the magnet track does not vary 100% sinusoidally along its length: only in that hypothetical case would the sinusoidal motor current yield a position-independent $K_f$. $K_f$ is the force per unit RMS current. We will call the ripple on $K_f$ the linear ripple, because the force deviation scales with current.

In addition, the interaction between the salient teeth of an Iron Core motor produces a force that is largely independent of motor current (known as cogging or Detent Force); this force is completely absent from Ironless motors.

Both types of motor ripple require special techniques to be incorporated into the system stability calculation. However, compensating the linear ripple requires much less bandwidth from the PID control. It is the cogging that presents the largest practical difficulties in a real-world application.

## III. SPLITTING UP MOTOR RIPPLE

In general, it can be said that a better understanding of the total motor ripple will lead to a better parametrized model. True understanding of a phenomenon is only possible if one is able to simulate it. Three degrees of complexity are possible for these calculations:

- various analytical approaches
- “steady state” FEM simulations
- FEM simulations including various hysteretic effects

For the “steady state” simulations, the assumption is that the system’s state is determined fully by the position and the motor current. In reality, the thrust of the motor is also dependent on its history. Loosely grouped under “hysteretic effects”, this is an order of magnitude harder to calculate, and is a subject of ongoing research.

“Steady state” FEM simulations are by far the most commonly used method and are the focus of this paper. Within the constraints of this method, accounting for cogging and linear motor ripple separately will lead to a great improvement in the parametrized model, especially for low motor current. In the extreme case that the target motor force is smaller than the cogging, the required current may actually be negative for a positive force, and vice versa, depending on the position.

The following conditions are necessary and sufficient for splitting up the total motor ripple into its constituent components:

- all forces/torques depend *only* on motor current and position
- linear ripple will scale with current, for both positive and negative currents
- cogging may depend on current level (as a result of magnetic saturation effects in steel), but its first order approximation will be independent of current
- friction will only depend on the direction of movement.

The general idea behind the method for quantifying components of the total motor ripple is doing double measurements. The direction of motion can be either forward or backwards, and the force can be directed either forward or backwards, see Fig. 1.

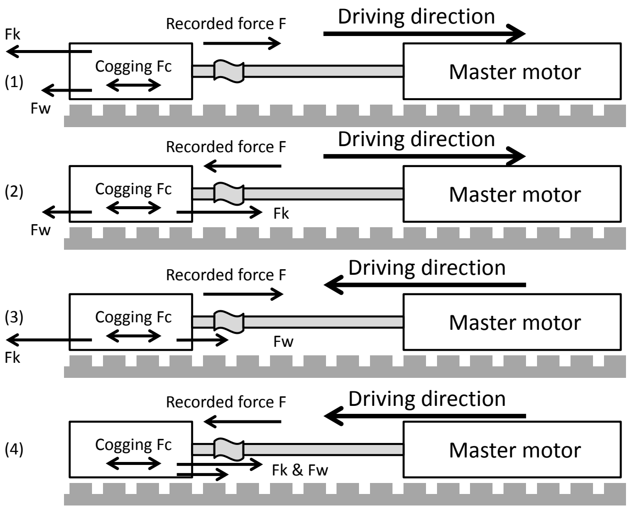


Fig. 1. Overview, in the case of a linear motor, of four measurement options, generated by positive/negative direction of movement and positive/negative direction of force. The direction of motion is shown. $F_c$ is cogging, $F_k$ is motor force (which includes the linear ripple) and $F_w$ is friction. The force F is measured by a sensor, indicated by the S-shape. The quandary of how to move left while exerting a force to the right is solved by using a larger master motor (on the right) to force the motor under test (on the left) in the direction of travel at constant speed.

Applying linear algebra to the use cases in Fig. 1 allows us to solve for all three forces: the motor force (which includes the linear ripple), the cogging and the friction. 4 equations with 3 unknowns constitute an overdetermined linear system. In this case, this means that there are two ways, two equations, for calculating friction and cogging. Only one each is used here:

- for quantifying cogging, one adds the exerted motor force under the two following conditions:
  - both motor force (for a given current) and friction are negative, meaning motion is in positive direction (case 1)
  - both motor force and friction are positive, meaning motion is in negative direction (case 4)
- for quantifying friction, one subtracts the exerted motor force under the following two conditions:
  - motor force in negative direction, friction negative, meaning motion is in positive direction (case 3)
  - motor force in negative direction, friction negative, meaning motion is in positive direction (case 1)
- subtracting both cogging and friction from the exerted motor force yields the sum of the average motor force and the linear ripple. One may obtain the average motor force by averaging over an integer number of electrical cycle lengths.

## IV. Qualititative Description of the Ripple

If four measurements (or simulations) are performed with a linear motor in positive/negative direction of motion, with positive/negative constant current, an example of the possible results is shown in Fig. 2.

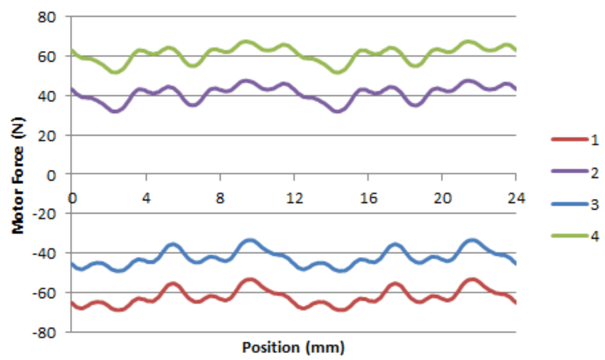


Fig. 2. Force as a function of position for low motor current, in the case of a linear motor, of four measurement options, generated by positive/negative direction of movement and positive/negative direction of force.

The simulation in Fig. 2 was performed for a relatively low motor current, with 10 N artificial friction, which can be directly identified from the image as half the distance between the top two curves. This, and the cogging, can be seen in Fig. 3.

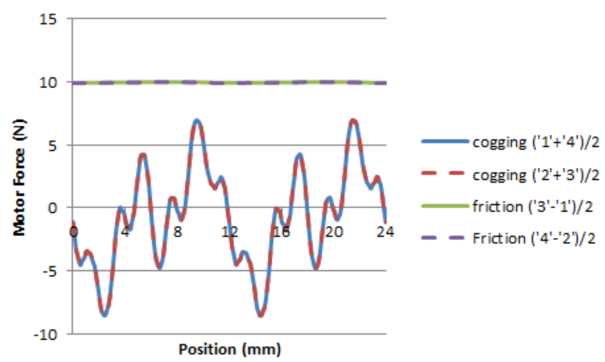


Fig. 3. Cogging and friction for low motor current, calculated by adding/subtracting datasets from Fig 2. This can be done two ways, so that there are two sets of two curves overlying each other.

The first observation that can be made when this operation is performed for a range of motor currents, is that the linear ripple is not the only thing that varies with current: the cogging changes both qualitatively and quantitatively. This is illustrated by Fig. 4, which shows the cogging of the same motor at high current.

The explanation why the cogging depends on the motor current is found in magnetic saturation effects in the steel. These influence the effective reluctance that the magnetic flux from the permanent magnets finds on its way through the motor laminations.

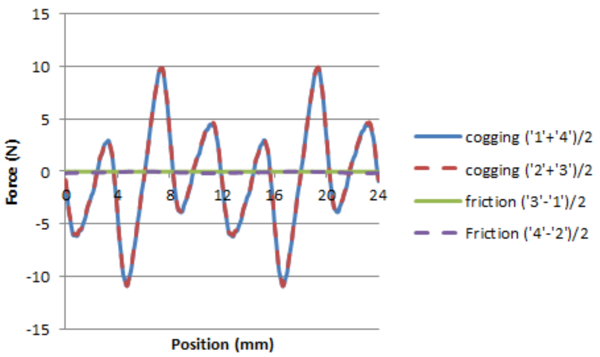


Fig. 4. Cogging and friction for high motor current, calculated by adding/subtracting datasets similar to Fig 2, but for high current. The simulations were performed without artificial friction.

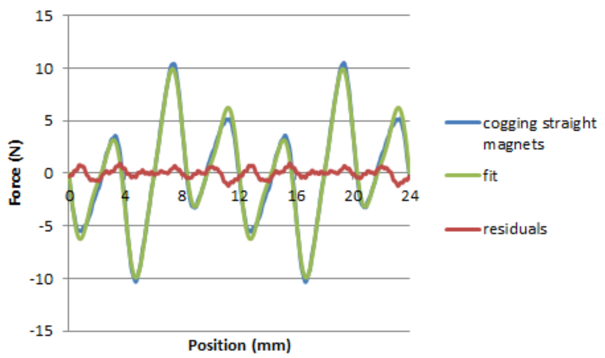


Fig. 5. Cogging for high motor current, fitted with a function composed of 4 harmonics of the base 24 mm: 12, 6, 4 and 2 mm. Why cogging is referred to as "cogging straight magnets" will become clear later in the text. Note that all harmonics are "sines" with phase zero at position 0 mm.

Comparing Fig. 3 to Fig. 4 begs the question of the composition of the ripple. Because it has to be periodic, it should be possible to "decompose" it into constituent harmonics. This is known as harmonic analysis, and is illustrated in Fig. 5, using the data from Fig. 4 at high motor current.

As it turns out, each of the constituent harmonics depends on the current in a different way. For some motors, all cogging harmonics share the same phase, but this is not always the case. Even for these motors, the equivalent decomposition of the linear ripple leads to harmonics that have a different phase (different from the cogging harmonics), see Fig 6. This illustrates the difficulty that a parametrized model will have that does not take the cogging and linear ripple both, independently, into account.

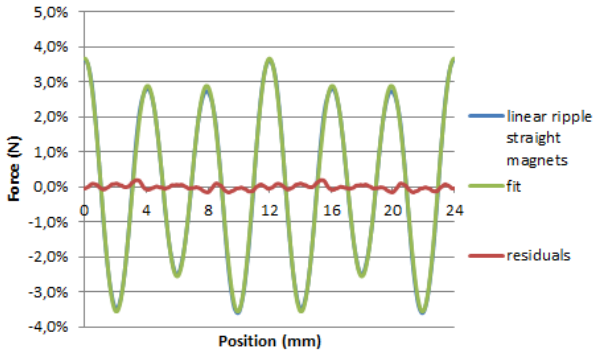


Fig. 6. Linear ripple for high motor current, fitted with a function composed of 4 harmonics of the base 24 mm: 12, 6, 4 and 2 mm. Note that all harmonics are "cosines" with phase zero at position 0 mm. This means there is a 90° phase difference with the cogging.

The amplitude of each constituent harmonic is a function of motor current in a different way, and can become both positive and negative, as is illustrated in Fig. 7.

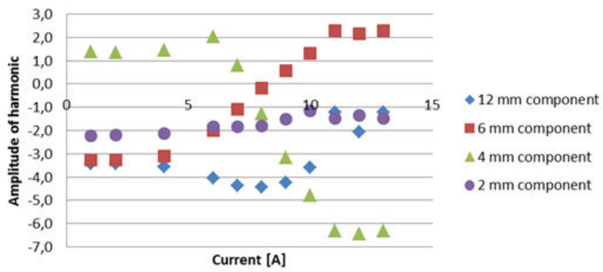


Fig. 7. The amplitude of cogging harmonics as a function of motor current.

The linear ripple harmonics follow a totally different pattern, see Fig. 8.

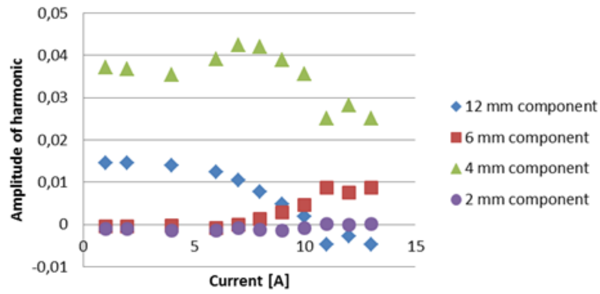


Fig. 8. The amplitude of linear ripple harmonics as a function of motor current. The 4 mm component is dominant.

We can now build a model of the behavior of the motor by taking the following components into account:

- four cogging harmonics, the amplitudes of which vary according to Fig. 7

- an average motor force which scales with current, including saturation
- four linear ripple harmonics, the amplitudes of which vary according to Fig. 8

As is evidenced by the small residuals in Fig. 5 and Fig. 6, this harmonic model accurately predicts the behavior of the motor in FEM simulation.

## V. Simulation Refinements

Two more simulation refinements will be discussed below.

### A. *Skewed magnets or teeth*

A well-known technique for reducing cogging is not placing the magnets perfectly perpendicular to the driving direction (||||) but rather under a small angle, in a skewed (////) or double-skewed (>>>>) orientation.

The effect of this technique on cogging can be approximated by smoothing the cogging curve with a rectangular kernel. The effect on any particular cogging harmonic is large if the kernel is wider than the period, small otherwise.

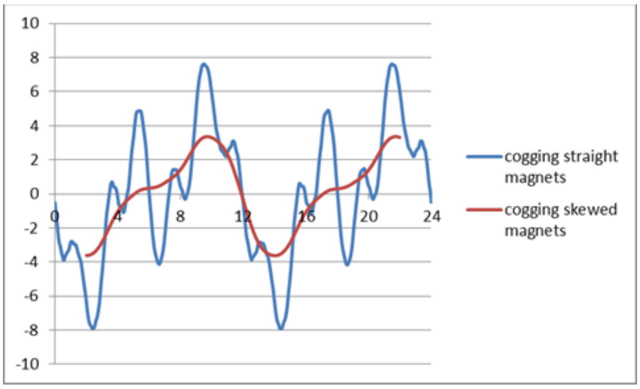


Fig. 9. The approximate effect of skewed magnets on the cogging. Mainly the higher harmonics are reduced.

As can be seen from Fig. 9, the effect of skewed magnets on the cogging is generally large.

Another option is to skew the teeth of the lamination stack rather than the magnets, which has the same effect.

### B. *Non-uniform magnets*

All previously discussed effects are part of the ideal ripple of the motor. These are present even in the ideal case, i.e. production of the motor with perfectly uniform materials and zero positioning and size tolerances.

In reality, these tolerances lead to a random distribution on a number of parameters, the effect of which can be simulated. Of course, it is to be expected that the cogging will be increased by these influences.

Interestingly, the effect of magnet strength being not uniform, but rather a set of random variates, is not only to increase the amplitude of the cogging constituent harmonics, but it also causes the appearance of a new harmonic, which corresponds to the tooth pitch rather than being a subharmonic of the magnet pitch.

Because the simulated motor places three teeth over four magnets, the tooth pitch of a motor with 24 mm electrical cycle (north-north pitch) is 16 mm. As can be seen in Fig. 10, a fluctuating 16 mm harmonic is clearly visible in the simulated cogging. To make the effect more clearly visible to the naked eye, the simulations were performed in this case with unrealistically large tolerances.

Because the tooth pitch harmonic (16 mm) fluctuates when the motor moves from (random) magnet to magnet, it cannot be neatly quantified. It depends on the set of random variates that was chosen for any particular simulation.

In a real motor, in addition to the harmonics that follow from the motor design (in this case 12, 6, 4 and 2 mm on an electrical cycle of 24 mm) we can expect one more harmonic: the tooth pitch, in this case 16 mm. The amplitude of this harmonic will depend on motor production processes, and will vary along the length of the motor track.

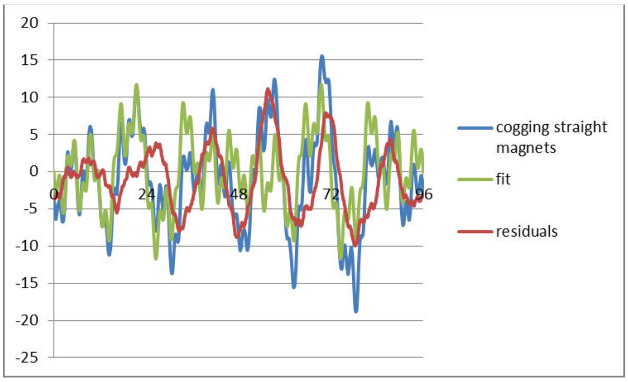


Fig. 10. Simulated cogging in the presence of (very large) non-uniform randomly distributed effects on magnet strength and position. The main component of the residuals repeats 6 times over 96 mm, which corresponds to 16 mm. This harmonic (tooth pitch) was not present in simulation of the ideal ripple.

## VI. Measurements

Measurements were performed on the same motor type as was used for the previous simulations. The results can be seen in Fig. 11.

At present, the practical difficulties in measuring force, position, speed and current simultaneously with sufficient accuracy do not allow us to perform frequency analysis with confidence. A new measurement setup is under development which should address this issue.

## VII. Parametrized Model

The considerations described in section 0 show us that even in an ideal system, where motor dimensions have no tolerances and magnets are perfectly uniform, the motor ripple shows complex behavior that cannot be easily linearized.

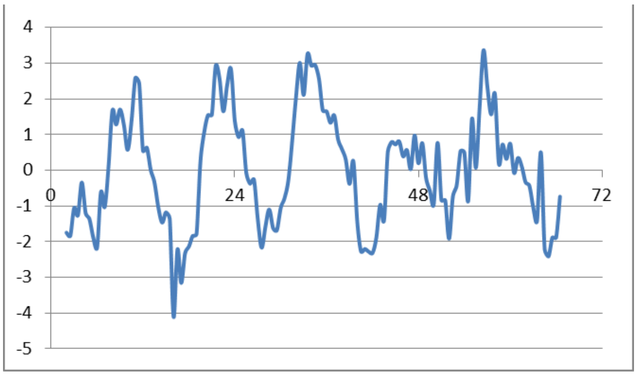


Fig. 11. Measured cogging profile. The achieved accuracy was not sufficient to allow frequency analysis, but it seems dominated by the 12 mm harmonic.

### A. *Example model*

As an example, we will compare the behavior of a motor as captured in an harmonic model in section 0 to that of a simplified model:

- the k-factor $k_f = \bar{F}/_I$, being the relation between current $I$ and average motor force $\bar{F}$, to be determined across the entire current range
- cogging, as determined at motor current $I = 0$ $A_{RMS}$, and assumed to be constant across the entire current range
- the linear ripple, as determined for a single motor current ($I = 4$ $A_{RMS}$ in Fig. 12), by determining total motor ripple and subtracting the cogging as determined previously for $I = 0$ $A_{RMS}$, and scaling across the entire current range.

Note that this model is already very advanced, because it takes cogging and linear ripple separately into account. It does this in the only way that is accessible to a researcher that is unfamiliar with the analysis method in Fig. 1, by determining cogging at $I = 0$ $A_{RMS}$ and linear ripple at some other current. It can be shown that any model taking less information into account than this one will deviate strongly for either high or for low motor current.

The formula for this simplified model will be, with $x$ the position and $F$ the "actual" motor force (as simulated in section 0):

$$F_{simplified}(I,x) = [F(4A,x) - F(0A,x)] \cdot \frac{I}{4A} \cdot \frac{k_f(I)}{k_f(4A)} + F(0A,x)$$

The deviation between this model and the actual force is shown in Fig. 12.

As we saw in section 0, both the linear ripple and the cogging change drastically for higher currents, presumably due to saturation effects. This is the reason that the largest deviations in Fig. 12 are seen for high current. Naturally, because the simplified model was based on a measurement for $I = 4$ $A_{RMS}$, the deviation is zero for this current.

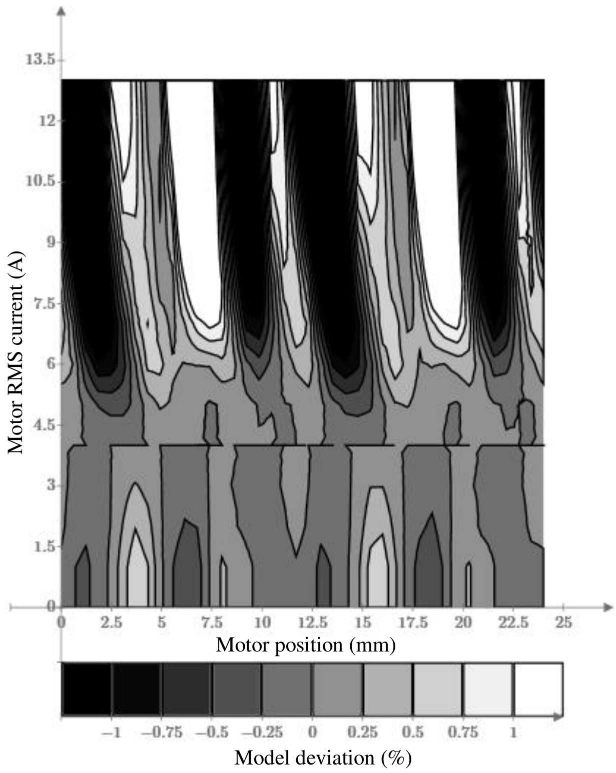


Fig. 12. Deviation, in percent, between the actual motor force and the force, predicted by a simplified model that is illustrative of the current state of the art. Simplified model inputs include cogging at zero motor current and total motor ripple at 4 $A_{RMS}$.

It is interesting to see that the model also shows a small deviation for low motor current. The simplified model assumes that cogging is independent of current, and linear ripple scales with current. Below 4 $A_{RMS}$, as can be seen from Fig. 7 and Fig. 8, this is not an unreasonable assumption. However, because cogging and ripple are not in phase with each other, small variations lead to large deviations. This emphasizes the need to independently determine both cogging and linear ripple.

In conclusion, there is a need for a certain amount of detail in the parametrized model, if it is to succeed in accurately predicting the motor's behavior. Feed-forward can then be used to improve the system's performance.

### B. *Types of models*

As to the nature of the parametrized model, our analysis shows that the effects of cogging and linear ripple can be clearly separated. It follows that they *should* be separated, in order for the model to be accurate across the full range of motor currents.

In short, there are three options for the model:

- Measure cogging at zero current, ignore linear ripple and ignore the difference in cogging for low and high current.
- Measure cogging across the range of currents, ignore linear ripple.

- Measure both cogging and linear ripple across the range of currents.

The first option (cogging only) has been successfully applied in the field. However, comparing Fig. 3 to Fig. 4, the performance of the resulting feed-forward system cannot be impressive at high current, because cogging is *not* constant.

The second option offers significant benefits, because it allows for better cancellation of the constant term, the cogging. A standard PID control is far more successful at compensating for the linear ripple, for the very reason that it is linear. This is illustrated by the fact that a standard method for improving motion quality in a system is to replace iron core by ironless motors. These have zero cogging, but comparable linear ripple. For a typical application, the resulting performance (for example in terms of the speed ripple) using a standard PID control is already sufficient without resorting to feed-forward.

The third option is the most complex. Based on the currently available measurement results, we cannot yet say whether the effect of random distributions is dominant or not. If it is not, a fully parametrized model could be a very good solution.

Even if random distributions are the dominant effect, the two kinds of ripple (cogging and linear) must be separated in order to give the best predictive value of the model for each value of the current, starting from a finite set of currents for which the ripple was measured.

## VIII. Conclusion

A method has been presented to separate two types of position-dependent parasitic force: cogging and linear ripple. By analyzing a simulation using this method, an enormous amount of detail becomes available.

This makes it possible to generate a harmonic motor model with realistically complex behavior in terms of analytical functions. Because the two types of ripple are out of phase with each other, it can be shown that any successful model must take the two types into account separately.

In measurement, higher accuracy is required than what is currently available to the authors, before a similar analysis can be made of a real motor under operating conditions.

Regardless of the outcome of further experiments, the method for splitting up the motor ripple into a current independent and a current dependent fraction is crucial for formulating an optimum model from a limited amount of measurement data.

## Acknowledgment

The author would like to acknowledge Peter Krechting, previously at Tecnotion but now working for Demcon in Enschede (NL), for having provided the key for the decomposition of the ripple into cogging and linear ripple.

## References

[1] S. Devasia, ”Robust Inversion-based Feedforward Controllers for Output Tracking under Plant Uncertainty”. Proc. of the American Control Conference, 2000, pp. 497-502.

[2] M. Boerlage, M. Steinbuch, P. Lambrechts, and M. van de Wal, “Model-based feedforward for motion systems,” in Proc. IEEE Conf. Control Applications 2, Istanbul, Turkey, 2003, pp. 1158–1163.